ISSN 1512-1461

UDC 538.9: Condensed matter Physics, Solid state Physics, Theoretical Condensed matter Physics

MAGNETIC DIPOLE INTERACTION AND TOTAL MAGNETIC ENERGY OF LITHIUM FERRITE THIN FILMS

[1]P. Samarasekara, [2]C. K.D. Sirimanna
[1,2] Department of Physics, University of Peradeniya, Peradeniya, Sri Lanka

Abstract
The classical Heisenberg Hamiltonian was employed to investigate the total magnetic energy of Lithium ferrite thin films. The short range magnetic dipole interactions between spins within one unit cell and the interactions between spins in two adjacent unit cells have been determined in order to find the total magnetic energy of lithium ferrite films. Only the spin pairs with separation less than cell constant have been taken into account to calculate dipole interaction and spin exchange interaction. Theoretically several easy and hard directions of lithium ferrite film were found for one set of energy parameters included in our modified Heisenberg Hamiltonian. The dependence of total magnetic energy of a lithium ferrite film on number of unit cells, spin exchange interaction, dipole interaction, second order magnetic anisotropy, fourth order magnetic anisotropy, internal applied magnetic field and stress induced magnetic anisotropy has been explained in this manuscript.

Keywords: *magnetic dipole interactions, ferrites, Heisenberg Hamiltonian, thin films*

1. Introduction:

Lithium Ferrite ($Li_{0.5}Fe_{2.5}O_4$) is a potential candidate in applications of magnetic memory devices, monolithic microwave integrated circuits and microwave devices. Polycrystalline thin films of lithium ferrite mixed with Mn have been synthesized on Al_2O_3 polycrystalline substrates using rf sputtering [1]. Easy axis oriented lithium ferrite films mixed with Mn have been fabricated on single crystal Al_2O_3 substrates using pulsed laser deposition technique [2]. In all these cases, the magnetic properties of films depend on the stress of the films induced within cooling and heating process. The crystal structure of lithium ferrite has been explained previously [3]. Magnetic properties of lithium ferrite nanoparticles with a core/shell structure have been investigated [4]. Infrared spectral properties of Magnesium and Aluminum co-substituted Lithium ferrites have been studied [5]. Influence of substrate on the octahedral site order of Structural and magnetic properties of Lithium ferrite thin films have been investigated [6]. The effect of Dipole and Anisotropic Hyperfine Fields on NMR of Fe in Lithium Ferrite has been studied [7].

For the first time, the short range magnetic dipole interaction of Lithium ferrite thin films have been explained in this manuscript. Previously the magnetic dipole interactions of nickel ferrite [8], barium ferrite [9] and cobalt [10] films have been described by us. However, cobalt belongs to the ferromagnetic category. In all above cases, the total magnetic energy was also determined using the classical Heisenberg Hamiltonian modified by introducing fourth order magnetic anisotropy, stress induced anisotropy and demagnetization factor. In addition, spin exchange interaction, magnetic dipole interaction, second order magnetic anisotropy constant and applied magnetic field terms can be found in this classical Heisenberg Hamiltonian. The investigations of barium ferrite films were restricted to unperturbed Heisenberg Hamiltonian. However, the studies of Nickel ferrite films were extended to third order perturbed Heisenberg Hamiltonian. In addition, the total magnetic energy of cobalt film was determined using second order perturbed Heisenberg Hamiltonian. The technique used to calculate magnetic dipole interaction in our previous reports was employed to find the magnetic dipole interaction of Lithium ferrite films explained in this manuscript. Only the

ISSN 1512-1461

interactions between iron ions were taken into account, since the net magnetic moment of each lithium and oxygen ions is zero.

2. Model:

The modified classical Heisenberg Hamiltonian is given by

$$H= - J\sum_{m,n}\vec{S}_m.\vec{S}_n + \omega\sum_{m\neq n}\left(\frac{\vec{S}_m.\vec{S}_n}{r_{mn}^{\ 3}} - \frac{3(\vec{S}_m.\vec{r}_{mn})(\vec{r}_{mn}.\vec{S}_n)}{r_{mn}^{\ 5}}\right) - \sum_m D_{\lambda_m}^{\ (2)}(S_m^{\ z})^2 - \sum_m D_{\lambda_m}^{\ (4)}(S_m^{\ z})^4$$

$$- \sum_m \vec{H}.\vec{S}_m - \sum_m K_s Sin2\theta_m \qquad \textbf{(1)}$$

Here J, S, ω, $D^{(2)}$, $D^{(4)}$, H and K_s represent the spin exchange interaction, spin, long range dipole interaction, second order anisotropy, fourth order anisotropy, magnetic field inside film and stress induced anisotropy, respectively. In addition, θ is the angle between local magnetization (M) and the stress. Within a single domain, M is parallel to the spin. If stress is applied normal to the film plane, then θ_m is the angle between the normal to the film plane and the local spin. Here the last term indicates the change of magnetic energy under the influence of a stress. K_s depends on the product of magnetostriction coefficient (λ_s) and the stress (σ). K_s can be positive or negative depending on the type of stress whether it is compressive or tensile. Integer m and n denote the indices of planes, and they vary from 1 to N for a film with N number of layers. First, second, third and fourth terms represent the spin exchange interaction, magnetic dipole interaction, second order anisotropy and fourth order anisotropy, respectively. Here $\vec{S}_i$ is a spin vector at point $\vec{r}_i$ in layer λ_i. Therefore the ground state energy will be calculated per spin with Z-axis normal to film plane. The total magnetic energy per unit spin of Fe^{3+} will be determined. The demagnetization factor was not considered in this study.

In Lithium ferrite structure, only the Fe^{3+} ions contribute to magnetic moment. Due to the unavailability of unpaired electrons, Li^+ ions don't have any net magnetic moment. Fe^{3+} ions occupy octahedral and tetrahedral sites of the lattice as given in table 1.

Layer	Atom number	Coordinates		
		x	y	z
A1	$A1_1$	0	0	0
	$A1_2$	1	0	0
	$A1_3$	0	1	0
	$A1_4$	1	1	0
	$A1_5$	0.5	0.5	0
B1	$B1_1$	0.625	0.125	0.125
	$B1_2$	0.375	0.875	0.125
	$B1_3$	0.125	0.625	0.125
A2	$A2_1$	0.25	0.25	0.25
	$A2_2$	0.75	0.75	0.25
B2	$B2_1$	0.625	0.375	0.375
	$B2_2$	0.375	0.625	0.375
	$B2_3$	0.875	0.125	0.375
A3	$A3_1$	0.5	0	0.5
	$A3_2$	0	0.5	0.5
	$A3_3$	1	0.5	0.5
	$A3_4$	0.5	1	0.5

ISSN 1512-1461

B3	$B3_1$	0.125	0.125	0.625
	$B3_2$	0.875	0.875	0.625
	$B3_3$	0.375	0.375	0.625
A4	$A4_1$	0.75	0.25	0.75
	$A4_2$	0.25	0.75	0.75
B4	$B4_1$	0.625	0.875	0.875
	$B4_2$	0.875	0.625	0.875
	$B4_3$	0.125	0.375	0.875
A5	$A5_1$	0	0	1
	$A5_2$	1	0	1
	$A5_3$	0	1	1
	$A5_4$	1	1	1
	$A5_5$	0.5	0.5	1

Table 1: Coordinates of Fe^{3+} ions in a unit cell corresponding to A (tetrahedral) and B (octahedral) sites.

First the spin exchange interactions between spins were determined as following. Only the interactions between spins separated by a distance less than the cell constant were considered. Spin exchange interactions were calculated for nearest spin neighbors within one cell and two adjacent cells as given in table 2.

	Interaction	**Number of Nearest Neighbors**	
		Within a unit cell	**Between two adjacent cells**
N_A	A-A	70	12
N_B	B-B	63	47
N_{AB}	A-B	230	63

Table 2: Number of nearest neighbors for each type of interaction.

By using the values given in table 2 and the first term in equation 1, the exchange interaction energy within a unit cell was found as 87J. Similarly the exchange interaction energy between two adjacent unit cells can be expressed as 4J. If there are N number of unit cells in the Lithium ferrite film in z direction, there are (N-1) adjacent cell combinations within the film. Therefore, the total exchange interaction energy can be written as 87NJ+4(N-1)J.

The magnetic dipole interaction energy between nearest spins (S_i and S_j) was determined using following equation and matrix.

$$E = \omega \vec{S}_i . W(r_{ij}) . \vec{S}_j \quad \textbf{(2)}$$

$$\text{Here } W(r) = \frac{1}{r^3}\begin{pmatrix} 1-3\hat{r}_x^{\,2} & -3\hat{r}_y\hat{r}_x & -3\hat{r}_z\hat{r}_x \\ -3\hat{r}_x\hat{r}_y & 1-3\hat{r}_y^{\,2} & -3\hat{r}_z\hat{r}_y \\ -3\hat{r}_x\hat{r}_z & -3\hat{r}_y\hat{r}_z & 1-3\hat{r}_z^{\,2} \end{pmatrix} \quad \textbf{(3)}$$

and $\omega = \dfrac{\mu_0 \mu^2}{4\pi a^3}$

ISSN 1512-1461

Only the interactions between spins separated by a distance less than the cell constant were considered. A film with (001) orientation of Lithium ferrite cell has been considered. As an example, the calculations of some elements of matrix appeared in equation 3 are given below. In layer A1 (bottom layer of the unit cell), five Ferric ions occupy $A1_1$(0, 0, 0), $A1_2$(1, 0, 0), $A1_3$(0, 1, 0), $A1_4$(1, 1, 0) and $A1_5$(0.5, 0.5, 0) sites [3]. Because the interactions between spins with separation less than the cell constant have been considered, only the $A1_1A1_5$, $A1_2A1_5$, $A1_3A1_5$ and $A1_4A1_5$ spin interactions have been taken into account. For these spin interactions, individual and total matrix elements are given in table 3.

	W_{11}	$W_{12}=W_{21}$	$W_{13}=W_{31}$	W_{22}	$W_{23}=W_{32}$	W_{33}
$A1_1$, $A1_5$	-1.41421	-4.24264	0	-1.41421	0	2.828427
$A1_2$, $A1_5$	-1.41421	4.24264	0	-1.41421	0	2.828427
$A1_3$, $A1_5$	-1.41421	4.24264	0	-1.41421	0	2.828427
$A1_4$, $A1_5$	-1.41421	-4.24264	0	-1.41421	0	2.828427
Total	-5.65685	0	0	-5.65685	0	11.31371

Table 3: The individual and total dipole matrix elements ofA1 layer of the unit cell.

The spins of Fe ions in the second spin layer located at a distance “a/8” above the bottom layer of Lithium ferrite unit cell occupy $B1_1$(0.125, 0.625, 0.125), $B1_2$(0.375, 0.875, 0.125) and $B1_3$(0.625, 0.125, 0.125) sites [3]. Because of the separations between following interactions are less than the cell-constant, the spin interactions between $A1_1B1_1$, $A1_1B1_2$, $A1_1B1_3$, $A1_2B1_1$, $A1_3B1_2$, $A1_3B1_3$, $A1_4B1_1$, $A1_4B1_2$, $A1_4B1_3$, $A1_5B1_1$, $A1_5B1_2$ and $A1_5B1_3$ were considered for this calculations. The individual and total dipole matrix elements of these interactions are given in table 4.

	W_{11}	$W_{12}=W_{21}$	$W_{13}=W_{31}$	W_{22}	$W_{23}=W_{32}$	W_{33}
$A1_1$, $B1_1$	-6.48786	-2.02746	-2.02746	3.24393	-0.40549	3.24393
$A1_1$, $B1_2$	0.61276	-1.20637	-0.17234	-1.68509	-0.40212	1.07233
$A1_1$, $B1_3$	3.24393	-2.02746	-0.40549	-6.48786	-2.02746	3.24393
$A1_2$, $B1_1$	-20.41307	11.48235	11.48235	10.20653	-3.82745	10.20653
$A1_3$, $B1_2$	-20.41307	11.48235	-11.48235	10.20653	3.82745	10.20653
$A1_3$, $B1_3$	10.20653	11.48235	-3.82745	-20.41307	11.48235	10.20653
$A1_4$, $B1_1$	0.61276	-1.20637	0.17234	-1.68509	0.40212	1.07233
$A1_4$, $B1_2$	-6.48786	-2.02746	2.02746	3.24393	0.40549	3.24393
$A1_4$, $B1_3$	-1.68509	-1.20637	0.40212	0.61276	0.17234	1.07233
$A1_5$, $B1_1$	10.20653	11.48235	-3.82745	-20.41307	11.48235	10.20653
$A1_5$, $B1_2$	10.20653	11.48235	3.82745	-20.41307	-11.48235	10.20653
$A1_5$, $B1_3$	-20.41307	11.48235	11.48235	10.20653	-3.82745	10.20653
Total	-40.81096	59.19261	7.65153	-33.37702	5.79978	74.18798

Table 4: The individual and total dipole matrix elements for the interaction between A1andB1 layer of the unit cell.

In a similar method, all the matrix elements for adjacent spin layers were calculated. The total matrix elements for the spins in adjacent layers within one unit cell are given table 5. Similarly the dipole interactions for next nearest layers in the cell were calculated.

Layer	Z	W_{11}	$W_{12}=W_{21}$	$W_{13}=W_{31}$	W_{22}	$W_{23}=W_{32}$	W_{33}
A1	4	-5.65685	0	0	-5.65685	0	11.31371
A1 and	12	-40.81096	59.19261	7.65153	-33.37702	5.79978	74.18798

ISSN 1512-1461

B1							
B1	3	-11.31122	-27.87701	0	-16.16848	0	27.47970
B1 and A2	6	-30.61960	28.36467	-5.85491	-9.73180	11.07686	40.35140
A2	1	-1.41421	-4.24264	0	-1.41421	0	2.82843
A2 and B2	6	-23.65700	-41.87448	-2.43295	-23.65700	2.43295	47.31400
B2	3	-24.04163	72.12489	0	-24.04163	0	48.08326
B2 and A3	12	-38.17979	-58.37153	8.22936	-38.17979	-8.22936	76.35958
A3	4	-5.65685	0	0	-5.65685	0	11.31371
A3 and B3	12	-36.00819	60.01370	-5.22195	-36.00819	-5.22195	72.01638
B3	5	-12.72792	-38.18377	0	-12.72792	0	25.45584
B3 and A4	6	-16.69440	14.85487	-7.65490	-16.69440	-7.65490	33.38880
A4	1	-1.41421	4.24264	0	-1.41421	0	2.82843
A4 and B4	6	-9.73180	-28.36467	-11.07686	-30.61960	-5.85491	40.35140
B4	3	-16.16848	27.87701	0	-11.31122	0	27.47970
B4 and A5	12	-33.37702	-59.19261	-5.79978	-40.81096	7.65153	74.18798

Table 5: The number of nearest neighbors and matrix elements of dipole tensor for each layer and two nearest layers with one unit cell.

Dipole interactions for spins in two adjacent cells are given in table 6.

Layer	Z	W_{11}	$W_{12}=W_{21}$	$W_{13}=W_{31}$	W_{22}	$W_{23}=W_{32}$	W_{33}
A2 and B1n	3	2.29785	0.51702	0.40212	2.75742	-1.20637	-5.05526
B2 and B1n	7	8.97557	1.57084	5.21379	8.19015	-0.78542	-17.16572
B2 and A2n	4	3.37018	-0.68935	0	3.37018	0	-6.74035
A3 and B1n	9	11.75873	-2.05185	0.73449	12.67787	-1.56336	-24.43661
A3 and A2n	4	5.10327	1.91372	0	5.10327	0	-10.20653
A3 and B2n	6	5.05526	-1.03403	-0.80425	5.05526	0.80425	-10.11053
B3 and B1n	9	7.96850	1.99839	1.57084	5.87404	-7.96167	-13.84254
B3 and A2n	4	10.40744	-2.35662	0.12721	10.40744	0.12721	-20.81488
B3 and	7	5.88409	-1.57084	-3.39231	6.66951	-1.03605	-12.55360

ISSN 1512-1461

B2n							
B3 and A3n	6	5.05526	1.03403	0.80425	5.05526	0.80425	-10.11053
A4 and B1n	6	30.61960	-5.78159	13.38260	28.59266	10.34220	-59.21226
A4 and A2n	4	2.82843	0	0	2.82843	0	-5.65685
A4 and B2n	5	11.08309	3.49678	-2.02746	11.08309	2.02746	-22.16618
A4 and A3n	4	5.10327	-1.91372	0	5.10327	0	-10.20653
A4 and B3n	2	1.68509	0.34468	0.80425	1.68509	0.80425	-3.37018
B4 and B1n	9	1.18771	-4.35465	40.11725	7.71968	-29.94233	-8.90740
B4 and A2n	6	28.59266	5.78159	-10.34220	30.61960	13.38260	-59.21226
B4 and B2n	9	9.18586	-4.96113	2.26019	9.18586	14.93439	-18.37172
B4 and A3n	9	12.67787	2.05185	1.56336	11.75873	0.73449	-24.43661
B4 and B3n	6	8.01561	-1.04723	-1.28668	8.01561	2.35626	-16.03123
B4 and A4n	3	2.75742	-0.51702	1.20637	2.29785	0.40212	-5.05526

Table 6: The number of nearest neighbors and matrix elements of dipole tensor for Fe^{3+} ions between nearest neighbor unit cell in z direction.

The final matrix elements for one cell are given in table 7.

	W_{11}	$W_{12}=W_{21}$	$W_{13}=W_{31}$	W_{22}	$W_{23}=W_{32}$	W_{33}
A-A	5.65685	0	0	5.65685	0	-11.31371
B-B	0	20.17463	20.17463	0	20.17463	0
A-B	0	-26.44766	-26.44766	0	-26.44766	0

Table 7: Total dipole matrix elements for A-A, B-B and A-B site interactions considered within the unit cell.

The final matrix elements for two adjacent cells are given in table 8.

	W_{11}	$W_{12}=W_{21}$	$W_{13}=W_{31}$	W_{22}	$W_{23}=W_{32}$	W_{33}
A-A	13.03496	0	0	13.03496	0	-26.06992
B-B	41.21734	-8.36462	44.48307	45.65486	-22.43482	-86.87220
A-B	120.30519	-0.23856	5.04649	120.30519	25.85484	-240.61038

Table 8: Total dipole matrix elements for A-A, B-B and A-B site interactions for nearest neighbor unit cells in z direction.

ISSN 1512-1461

After substituting these matrix elements in the matrix given in equation (3), the dipole matrix can be obtained. By substituting that dipole matrix in equation (2), the dipole interaction energy in each case can be found as following.
The total dipole moment for the spins within A layer can be given as

E^{dipole}_{A}= -11.31371ω(0.25+0.75cos2θ)

Similarly for all B type and A-B nearest neighbor interactions within the unit cell, the total dipole interaction energy can be given as

E^{dipole}_{B}= 20.174631ωsin2θ

E^{dipole}_{AB}= 26.44766ωsin2θ

Finally the total dipole interaction energy within the unit cell can be given as

$$E^{dipole}_{unit\ cell} = \omega(46.52229\sin2\theta - 2.82843 - 8.48528\cos2\theta) \quad \textbf{(4)}$$

Similarly for all A type, B type and A-B nearest neighbor interactions between two adjacent unit cells in z direction, the total dipole interaction energy can be given as

$E^{dipole}_{A\text{-}adj}$ = -26.06992ω(0.25+0.75cos2θ)

$E^{dipole}_{B\text{-}adj}$ = -ω(20.60867+ 22.42482sin2θ+66.26353cos2θ)

$E^{dipole}_{AB\text{-}adj}$ = ω(60.1526-25.85484sin2θ+180.45779cos2θ)

Therefore the total dipole interaction energy between two adjacent unit cells in z direction can be given as

$$E^{dipole}_{adj\text{-}cells} = \omega(33.02645-48.28966\sin2\theta+94.64182\cos2\theta) \quad \textbf{(5)}$$

If there is N number of unit cells in the Lithium ferrite film in z direction, then the total dipole interaction energy can be given as

$$E^{dipole}_{total} = NE^{dipole}_{unit\text{-}cell} + (N-1)E^{dipole}_{adj\text{-}cells} \quad \textbf{(6)}$$

By substituting equations (4) and (5) in equation (6), the total dipole interaction energy of a Lithium ferrite film with thickness Na (height of N cubic unit cells) in z direction can be given as,

E^{dipole}_{total} = Nω(46.62229sin2θ –2.82843 –8.48528cos2θ)
+(N-1) ω(33.02645-48.28966sin2θ+94.64182cos2θ) **(7)**

Then by substituting equation (7) in equation (1), the total energy per unit spin can be given as,

$$\begin{aligned} E(\theta) = {} & (91N-4)J \\ & + \omega\{N(46.62229\sin 2\theta - 2.82843 - 8.48528\cos 2\theta) \\ & + (N-1)(33.02645 - 48.28966\sin 2\theta + 94.64182\cos 2\theta)\} \\ & - \cos^2\theta \sum_{m=1}^{N} D_m^{(2)} - \cos^4\theta \sum_{m=1}^{N} D_m^{(4)} \\ & + 4N(H_{in}\sin\theta + H_{out}\cos\theta + K_s\sin 2\theta) \end{aligned}$$

Hence

$$\begin{aligned} \frac{E(\theta)}{\omega} = {} & (91N-4)\frac{J}{\omega} + N(46.62229\sin 2\theta - 2.82843 - 8.48528\cos 2\theta) \\ & + (N-1)(33.02645 - 48.28966\sin 2\theta + 94.64182\cos 2\theta) \\ & - \cos^2\theta \frac{\sum_{m=1}^{N} D_m^{(2)}}{\omega} - \cos^4\theta \frac{\sum_{m=1}^{N} D_m^{(4)}}{\omega} \\ & + 4N\left(\frac{H_{in}}{\omega}\sin\theta + \frac{H_{out}}{\omega}\cos\theta + \frac{K_s}{\omega}\sin 2\theta\right) \end{aligned}$$

ISSN 1512-1461

Following 2-D and 3-D graphs have been plotted using above final energy equation.

3. Results and discussion:

The 3-D graph of $\frac{E(\theta)}{\omega}$ versus $\frac{\sum_{m=1}^{N} D_m(2)}{\omega}$ and θ is given in figure 1. The variation of energy is most likely periodic. Values of other parameters were kept at

$$\frac{J}{\omega} = \frac{H_{in}}{\omega} = \frac{H_{out}}{\omega} = \frac{K_s}{\omega} = 10, N = 1000 \text{ and } \frac{\sum_{m=1}^{N} D_m(4)}{\omega} = 5$$

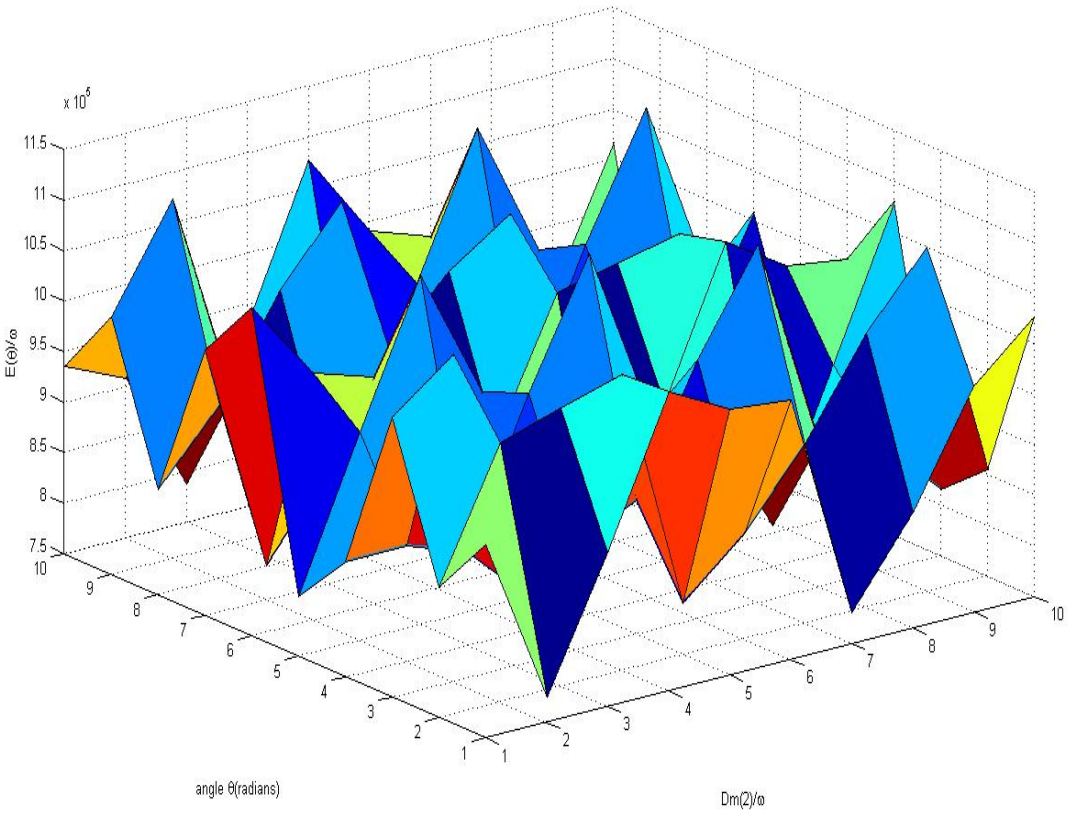

Figure 1: 3-D graph of $\frac{E(\theta)}{\omega}$ versus $\frac{\sum_{m=1}^{N} D_m(2)}{\omega}$ and θ for $\frac{J}{\omega} = \frac{H_{in}}{\omega} = \frac{H_{out}}{\omega} = \frac{K_s}{\omega} = 10, N = 1000 \text{ and } \frac{\sum_{m=1}^{N} D_m(4)}{\omega} = 5$.

By using the $\frac{\sum_{m=1}^{N} D_m(2)}{\omega}$ values for each of the maxima and minima of the 3D graph, the 2-D graphs of $\frac{E(\theta)}{\omega}$ versus θ were plotted in order to find easy and hard directions of magnetization. One of those graphs is shown in figure 2 for $\frac{\sum_{m=1}^{N} D_m(2)}{\omega}$ = 44 (one of the maximum energy points) and another graph is shown in figure 3 for $\frac{\sum_{m=1}^{N} D_m(2)}{\omega}$ = 55 (one of the minimum energy points). According to figure 2, the hard directions are 0.2, 3, 6.4 radians ----etc for given values of energy parameters. The easy directions are 1.6, 4.5, 7.9 radians ------etc from figure 3.

ISSN 1512-1461

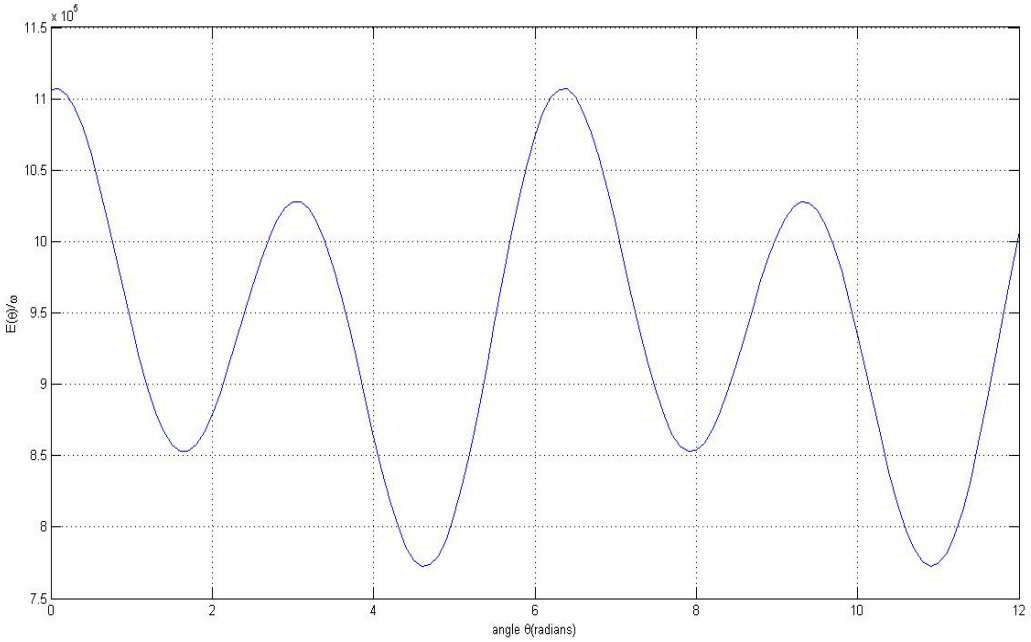

Figure 2: The graph of $\frac{E(\theta)}{\omega}$ versus θ at $\frac{\sum_{m=1}^{N} D_m(2)}{\omega}$= 44 (one of the maximum energy points in 3-D plot).

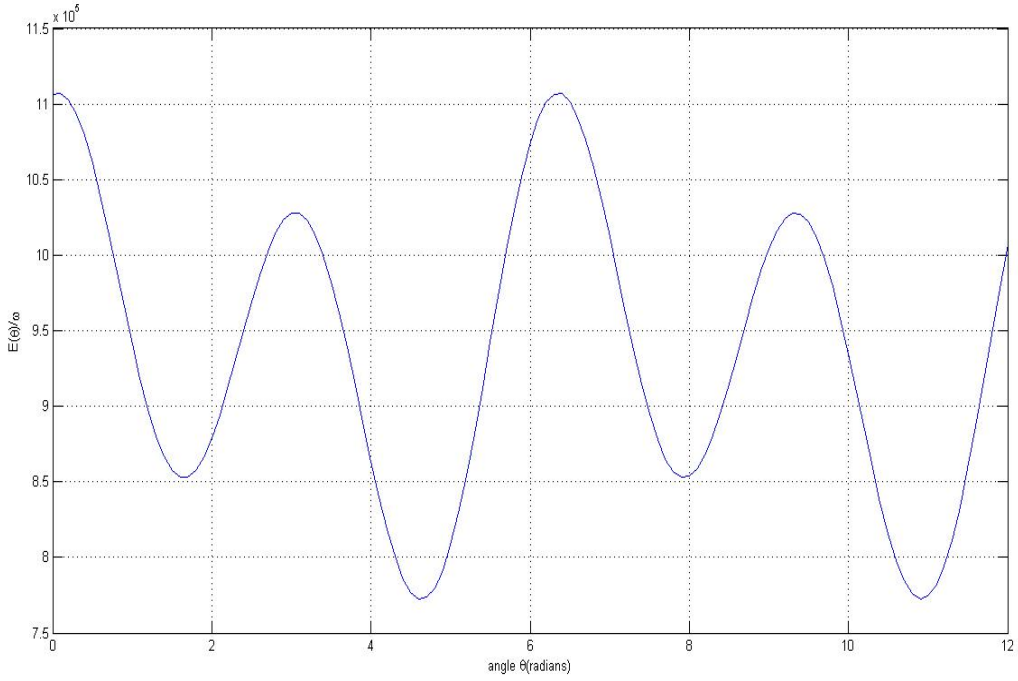

Figure 3: The graph of $\frac{E(\theta)}{\omega}$ versus θ at $\frac{\sum_{m=1}^{N} D_m(2)}{\omega}$= 55 (one of the minimum energy points in 3-D plot).

Curves given in figures 2 and 3 are slightly different. The variations of energy with other parameters have been also studied, and it has been summarized in the tale given in the conclusion part.

ISSN 1512-1461

4. Conclusion:

The total magnetic energy obtained using modified Heisenberg Hamiltonian varies periodically with energy parameters. The magnetic easy and hard directions were determined using 2-D and 3-D plots. The variation of energy is somewhat similar for $\frac{\sum_{m=1}^{N} Dm(2)}{\omega}$ and $\frac{\sum_{m=1}^{N} Dm(4)}{\omega}$. Higher variations could be observed for larger values of $\frac{H_{in}}{\omega}$, $\frac{H_{out}}{\omega}$ and $\frac{K_s}{\omega}$. When the number of layers or $\frac{J}{\omega}$ increases, the peak value of energy also increases. Changing $\frac{\sum_{m=1}^{N} Dm(2)}{\omega}$, $\frac{\sum_{m=1}^{N} Dm(4)}{\omega}$, $\frac{J}{\omega}$, $\frac{K_s}{\omega}$ or N does not change the easy axis or hard axis very much. But the angle of the hard axis increases with $\frac{H_{in}}{\omega}$, and the angle of the easy axis decreases with $\frac{H_{out}}{\omega}$.

Easy and hard directions for different energy parameters are given in following table.

Parameter							Easy axis	Hard axis
$\frac{\sum_{m=1}^{N} Dm(}{\omega}$	$\frac{\sum_{m=1}^{N} Dm(4)}{\omega}$	$\frac{H_{in}}{\omega}$	$\frac{H_{out}}{\omega}$	$\frac{J}{\omega}$	$\frac{K_s}{\omega}$	N		
0-100	5	10	10	10	10	1000	$265°17'$	$4°24'$
10	0-100	10	10	10	10	1000	$265°17'$	$3°50'$
10	5	0-100	10	10	10	1000	$265°51' - 267°$	$6°42' - 45$
10	5	10	0-100	10	10	1000	$230°54' - 261°$ 51’	$2°41' - 3°$
10	5	10	10	0-100	10	1000	$265°17' - 265°$	$3°50'$
10	5	10	10	10	0-100	1000	$265°51' - 268°$	$1°32' - 3°$
10	5	10	10	10	10	976-3000	$265°17'$	$4°24'$

Table 9: Variation of easy and hard axis with each of seven unknown parameters.

References:

1. P. Samarasekara and F.J. Cadieu, Chinese Journal of Physics (2001), 39(6), 635.
2. P. Samarasekara, Chinese Journal of Physics (2002), 40(6), 631.
3. A. I. Smolentsev, A.B. Meshalkia, N.V. Podberezskaya and A.B. Kaplun, Journal of Structural Chemistry (2008), 49 (5), 953.
4. N. Jovic, B. Antic, G. F. Goya and V. Spasojevic, Current Nanoscience (2012), 8(5), 651.
5. K.B. Modi, J.D. Gajera, M.P. Pandya, H.G. Vora and H.H. Joshi, Pramana Journal of Physics (2004), 62 (5), 1173.
6. Cihat Boyraz, Dipanjan Mazumdar, Milko Iliev, Vera Marinova, Jianxing Ma, Gopalan Srinivasan and Arunava Gupta, Applied Physics Letters (2011), 98, 012507.
7. V.D. Doroshev, V.A. Klochan, N.M. Kovtun and V.N. Seleznev, Physica Status solidi (1972), 9, 679.
8. P. Samarasekara, Electronic Journal of Theoretical Physics (2007), 4(15), 187.
9. P. Samarasekara and Udara Saparamadu, Georgian Electronic Scientific Journals: Physics (2013), 1(9), 10.
10. P. Samarasekara and Amila D. Ariyaratne, Research & Reviews: Journal of Physics- STM journals (2012), 1(1), 16.

Article received: 2014-01-13